Photoproduction of Neutral Pions in Hydrogen: Magnetic Analysis of Recoil Protons*

D. C. OAKLEY† AND R. L. WALKER
California Institute of Technology, Pasadena, California
(Received November 17, 1954)

The photoproduction of neutral pions from hydrogen has been studied by counting the recoil protons with a magnetic spectrometer and scintillation counters. The process has been studied between photon energies of 260 and 450 Mev and between center-of-momentum pion angles of 70° and 153°. The excitation functions show a resonance type shape with maxima at about 320 Mev. Angular distributions are analyzed in the form $A+B\cos\theta+C\cos^2\theta$ in the center-of-momentum system. The coefficient B, which gives the front-back asymmetry, is small at all energies; and the ratio $-A/C$ is 1.22 ± 0.10 at all energies between 295 and 450 Mev. The maximum cross section at 90° in the c.m. system is 26×10^{-30} cm²/steradian for 320-Mev photons. The total cross section divided by the square of the c.m. photon wavelength has a maximum near 340 Mev, and drops by nearly a factor of two at 450 Mev. These results are consistent with magnetic dipole and electric quadrupole absorption leading to a resonant state of the pion-nucleon system of angular momentum $\frac{3}{2}$ and isotopic spin $\frac{3}{2}$.

INTRODUCTION

THE photoproduction of neutral pions from hydrogen is one of the fundamental experiments to determine the nature of the pion-proton interaction. It is perhaps the least well known of the fundamental experiments, meson-proton scattering and photoproduction of pions from hydrogen. This work reports experimental work done at the California Institute of Technology's synchrotron on the photoproduction of neutral pions from hydrogen.

This reaction has shown[1–5] a marked difference from the positive pion photoproduction near threshold.[6] The positive pion photoproduction increases about as $(E_\gamma-E_T)^{\frac{1}{2}}$, where E_γ is the gamma-ray energy and E_T is the threshold of the reaction. The neutral production increases about as $(E_\gamma-E_T)^{\frac{3}{2}}$ near threshold and at 300 Mev is comparable with the positive production. Weak coupling theory predicts that neutral production should be much smaller than positive production. The energy dependence and nearly isotropic angular distribution of the positive pion photoproduction near threshold indicates a large S-state contribution to the cross section. The energy dependence and non-isotropic angular distribution of neutral pion photoproduction near threshold indicates very little S-state contribution and the large cross section near 300 Mev is suggestive of a resonance in the P-state contribution. Since strong coupling theory predicted a resonance, in pion-nucleon scattering, of the $P_{3/2}$ state with isotopic spin $\frac{3}{2}$, and experiments had shown an indication of this resonance, Brueckner and Case[7] suggested that this state might also be important in the photoproduction of pions. Brueckner and Watson[8] used this suggestion to calculate an excitation function.

Some general features of the possible angular distributions and energy dependence near threshold, based on angular momentum considerations, have been given by Feld[9] and by Watson[10] and Gell-Mann.[11] Watson[10] gives general relationships between photoproduction and meson-nucleon scattering. A "semi-phenomenological" theory relating photoproduction and scattering has been given by Ross,[12] which covers the energy range of the present experiment. Chew[13] has made calculations of meson scattering and photoproduction, using a cut-off theory.

Probably the most useful theory for the analysis of the experimental data is the phenomenological one of Gell-Mann and Watson,[11] as extended recently by Watson.[14] All such theories make an analysis in terms of matrix elements for photoproduction into states of definite angular momentum and isotopic spin. This means that a full comparison with experiment can only be made by combining data on charged and neutral pion production,—these involving different combinations of isotopic spin states. For this reason it is important to obtain cross sections for both positive and neutral pion production, whose absolute values may be compared. It is hoped that the present data, taken with the same magnetic spectrometer and same synchrotron beam as previous measurements of positive pion production[15] will fill this need, although the two sets of measurements were taken rather far apart in time.

* This work was supported in part by the U. S. Atomic Energy Commission.
† Now at University of California Radiation Laboratory, Livermore, California.
[1] Steinberger, Panofsky, and Steller, Phys. Rev. **78**, 802 (1950).
[2] Panofsky, Steinberger, and Steller, Phys. Rev. **86**, 180 (1952).
[3] A. Silverman and M. Stearns, Phys. Rev. **88**, 1225 (1952).
[4] Walker, Oakley, and Tollestrup, Phys. Rev. **89**, 1301 (1953).
[5] Goldschmidt-Clermont, Osborne, and Scott, Phys. Rev. **89**, 329 (1953); Phys. Rev. **97**, 188 (1955).
[6] See for example G. Bernardini and E. L. Goldwasser, Phys. Rev. **95**, 857 (1954).
[7] K. A. Brueckner and K. M. Case, Phys. Rev. **83**, 1141 (1951).
[8] K. A. Brueckner and K. M. Watson, Phys. Rev. **86**, 923 (1952).
[9] B. T. Feld, Phys. Rev. **89**, 330 (1953).
[10] K. M. Watson, Phys. Rev. **95**, 228 (1954).
[11] M. Gell-Mann and K. M. Watson, Ann. Rev. Nuc. Sci. (to be published).
[12] M. Ross, Phys. Rev. **94**, 454 (1954).
[13] Geoffrey F. Chew, Phys. Rev. **95**, 1669 (1954).
[14] K. M. Watson. Lectures at the California Institute of Technology during the summer, 1954.
[15] Walker, Teasdale, and Peterson, Phys. Rev. **92**, 1090 (1953). A complete report of these measurements will be published soon.

There have been four methods used to measure the reaction

$$\gamma+p\rightarrow p+\pi^0;\quad \pi^0\rightarrow 2\gamma.$$

(1) detect both gamma rays in coincidence,
(2) detect the proton and one gamma ray in coincidence,
(3) detect one gamma ray only,
(4) detect the proton only.

Steinberger, Panofsky, and Steller[1,2] used the first method in their work which pioneered the observation of this phenomenon and which demonstrated the existence of the neutral pion. This method had the advantage at that time of establishing the existence of the neutral pion and its mode of decay into two photons. Method 2 has been used by Silverman and Stearns[3] and later by Walker, Oakley, and Tollestrup.[4,16] This method suffers from counting rate difficulties and requires an accurate calibration of the efficiency of the gamma-ray counter for detecting at least one of the decay gamma rays from the neutral pion. Method 3 has been used by Cocconi and Silverman[17] for angular distributions and total cross section measurements even though the decay gamma rays are loosely correlated with the neutral pion. Method 4 has been used by Goldschmidt-Clermont, Osborne, and Scott[5] who counted the recoil protons by photographic plate techniques. Method 4 was also used in this experiment. The proton is identified at a laboratory angle by its momentum and its ionization loss in a scintillator. The experiment is capable of attaining good statistics, but requires proof that other processes are not contributing to the flux of protons.

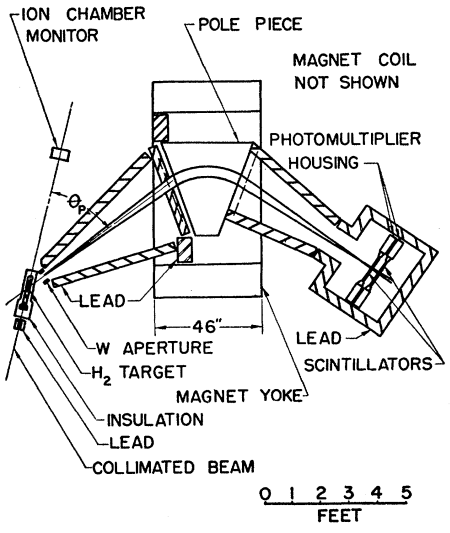

FIG. 1. Diagram of the magnetic spectrometer.

[16] Walker, Oakley, and Tollestrup, preceding paper [Phys. Rev. 97, 1279 (1955)].
[17] G. Cocconi and A. Silverman, Phys. Rev. 88, 1230 (1952).

APPARATUS

The apparatus used in this experiment is shown in Fig. 1. The 500-Mev bremsstrahlung beam of the CalTech synchrotron was collimated by a front lead collimator and two successive lead scrapers to eliminate the splatter from the walls of the front collimator. At the target, the beam was 3.8 cm in diameter.

The hydrogen target consisted of a steel flask of nominal thickness 0.030 inch, 2 inches in diameter, and 17 inches long, enclosed in a block of Styrafoam insulation 6×5 inches in cross section and most of the time further enclosed in a double polyethylene bag of 0.011-inch total thickness to keep water from condensing on the steel. Attached to the flask was a liquid nitrogen reservoir to cool the gas. The hydrogen was dried in a liquid nitrogen trap at each filling. The hydrogen was kept at a typical density of 0.032 gram/cm^3 by compressing the gas in the liquid nitrogen cooled flask to 2000 psi. The temperature was read periodically by comparing iron-constantan thermocouples attached to the flask with one immersed in boiling nitrogen. The Handbook of Chemistry and Physics was used for the calibration of the thermocouples. The density was found by interpolating the data of Johnson *et al.*[18] The density was read periodically and interpolated between readings.

There was considerable background counting rate at some of the settings. This rate was measured by taking runs with the hydrogen vented to the atmosphere or pumped below atmospheric pressure by a vacuum pump. Sufficient backgrounds were taken to give approximately the minimum statistical error in the hydrogen-background difference for a given total running time.

The wolfram slits define the volume of hydrogen used as a source. When looking at protons of momentum greater than could be directly measured by the spectrometer, carbon absorbers were placed at these slits to slow down the protons before they entered the magnet. By putting the absorber at the slits, the Coulomb multiple scattering out of the beam was cancelled by the scattering in. This was tested by using absorbers of larger atomic number and hence larger mean square scattering angle. These tests show that carbon is a safe absorber to use. Corrections have been made for the nuclear absorption by the absorbers, the target wall, and the air path, and for the nuclear scattering by the absorbers.

The counter house was placed 529 cm from the target for the "long focus" arrangement used at 12.5° and at 19.5°. It was placed 350 cm from the target for the "short focus" arrangement used at the other angles. The magnet was placed between the counter house and the target. The peak magnetic field of 15 kilogauss and the long-focus radius of curvature of 98 cm correspond

[18] Johnson, Bezman, Rubin, Swanson, Corak, and Rifkin, Atomic Energy Commission Report MDDC-850 (unpublished).

to protons of about 98 Mev and the short-focus radius of curvature of 72 cm to protons of about 54 Mev. The field of the magnet was calibrated by a proton moment apparatus, and the current was controlled by a current feedback system.

During the course of the experiment, it was found that the lead "bridges" used to shield the magnet aperture from stray particles were capable of scattering protons into the aperture that would not have gotten in otherwise. In the later portion of the experiment, the bridges were piled as shown in Fig. 1. The earlier portion had the bridges piled much closer to the particle trajectories. The effect of the position of these bridges will be discussed below under "Errors."

The counters were of two types. The thick counters used in the 12.5° setting were Lucite bottles of dimensions $1\times6\times9$ inches, with $\frac{1}{16}$ inch walls, filled with a liquid scintillator. Thin counters made of plastic, kindly furnished by the Los Alamos laboratory, were used in all the other settings. The front thin counter was $\frac{1}{4}\times6\times9$ inches and the back one was $\frac{1}{2}\times6\times9$ inches. Both sets of counters were surrounded by 0.001-inch bright aluminum for a reflector and by a slightly thicker layer of aluminum for light shielding.

The scintillators were viewed by one RCA 5819 photomultiplier tube at each end. The outputs of the two tubes on each scintillator were connected in parallel.

A seven-channel analyzer recorded the pulse height from the phototubes in the front counter. For the lowest photon energies, the associated protons have too little energy to traverse the first counter and register a count in the second. For these energies, the pulse heights in the front counter were recorded, without requiring a coincidence with the second. For higher energies when the protons could traverse the first counter and get sufficiently far into the second counter to count reliably, coincidences were required between the two counters to trigger a gating circuit which then reproduces the pulse height in the front counter. Sample pulse-height histograms from the first counter under these two conditions are shown in Fig. 2. Accidental coincidences were monitored by counting the coincidences between the first counter and a signal from the second counter delayed 0.8 microsecond. The accidental rate was always negligible.

The total energy in the bremsstrahlung beam was monitored by a Cornell type ionization chamber with the output integrated by a current integrator. This chamber has copper walls one inch in thickness, which is very close to the peak of the shower curve for a wide range of energies. The output is nearly proportional to the total energy, independent of the maximum energy of the beam. This ion chamber and current integrator have been calibrated by a pair spectrometer[19] and also by J. C. Keck using the shower method of Blocker, Kenny, and Panofsky.[20] The pair spectrometer measurement of the ion chamber calibration was $(4.75\pm0.13)\times10^{18}$ Mev/coulomb and the shower method measurement gave $(4.12\pm0.20)\times10^{-18}$ Mev/coulomb. The mean value 4.44×10^{18} Mev/coulomb, was used for this measurement.[21] The two calibrations are 3 standard deviations apart, but the discrepancy has not been found. An error of 7 percent is assigned to the beam calibration.

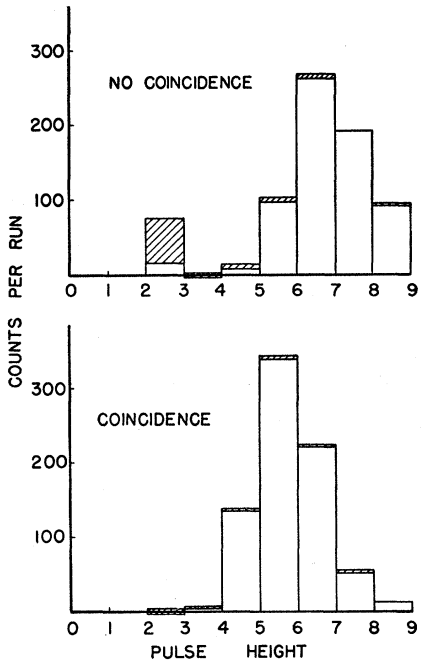

FIG. 2. Proton peaks in the pulse-height spectra from the first counter, with and without the requirement of a coincidence with the second counter. Cross-hatched areas represent backgrounds subtracted.

Room temperature and pressure and the peak energy of the synchrotron were monitored and corrections have been made for the effects of these on the number of ions collected from the ionization chamber.

RESULTS

Due to the size of the magnet and counter house and the need for restacking the lead bridges after each magnet moves, it was convenient to set the spectrometer in place and then make runs with different currents and absorbers, getting all runs, including backgrounds, before moving the magnet again. This procedure gives excitation functions for constant laboratory angles. The results are shown in Figs. 3 through 7 for 12.5°, 19.5°, 29°, 40.5°, and 50.3°, respectively. The cross sections are in the center of momentum system while the photon energies are in the laboratory system. Those

[19] D. H. Cooper, thesis, California Institute of Technology, 1954 (unpublished).

[20] Blocker, Kenny, and Panofsky, Phys. Rev. **79**, 419 (1950).

[21] Extrapolation of the mean value to 300-Mev bremsstrahlung gives 3.91×10^{18} Mev/coulomb. The calibration at Cornell University is 3.68×10^{18} Mev/coulomb.

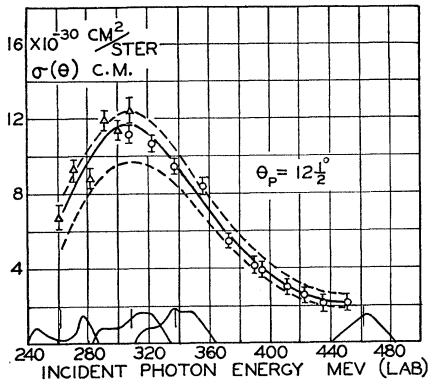

FIG. 3. Excitation function at 12.5° (lab). The differential cross section in the center-of-momentum system is shown as a function of the laboratory photon energy. Data shown by circles in this and the other excitation curves were obtained by requiring a coincidence between the two counters. Points indicated by triangles were obtained from counts in the first counter alone.

points having two errors have been obtained from the first set of experiments, with the lead bridges close to the proton trajectories; in which the protons were found to scatter from the bridges. A correction factor was determined from the ratio of the second set to the first set cross sections. The smaller errors are from the counting statistics, while the larger errors include the error in this correction factor. The entire 12.5° experiment, Fig. 3, is from the first set, with no correction factor, but large errors because of the uncertainty in this scattering effect. The points with only one error in the rest of the figures are from the second set. The triangles denote the points that could not make use of the coincidence technique of counting the protons, while the circles denote the use of coincidence between the two counters to trigger the gating circuit.

The energy resolution functions are shown at the bottom of each figure for various representative settings. These settings were chosen so that the shapes of the functions vary smoothly between the figures

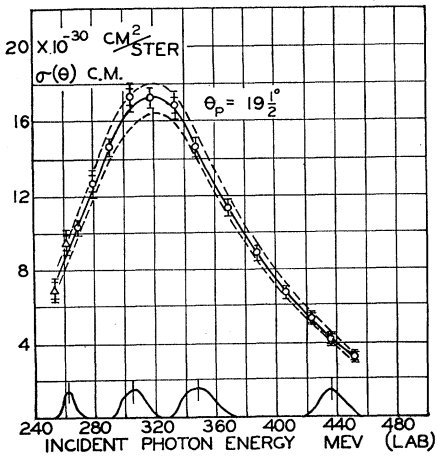

FIG. 4. Excitation function at 19.5° (lab).

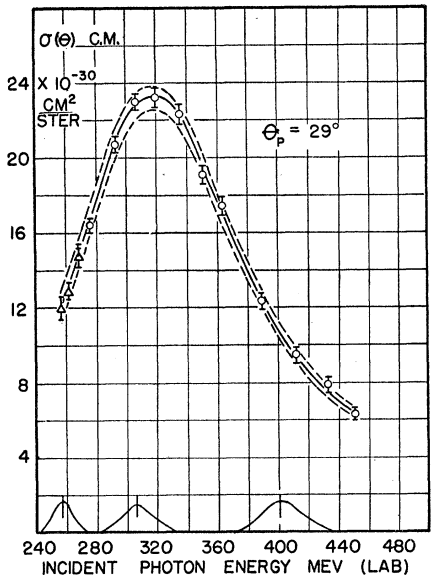

FIG. 5. Excitation function at 29° (lab).

shown. These resolution functions include the effects of the angular resolution as well as the momentum resolution. The unusual resolution functions in Fig. 3, 12.5°, are due to the target wall. At this angle, protons came through the cap of the target as well as the sides. The lower-energy peak is from those protons which came through the cap of the target, losing much less energy than those protons which came through the side wall, and which provide the higher-energy peak.

The errors on the points are standard deviations composed of statistical errors. The dotted curves

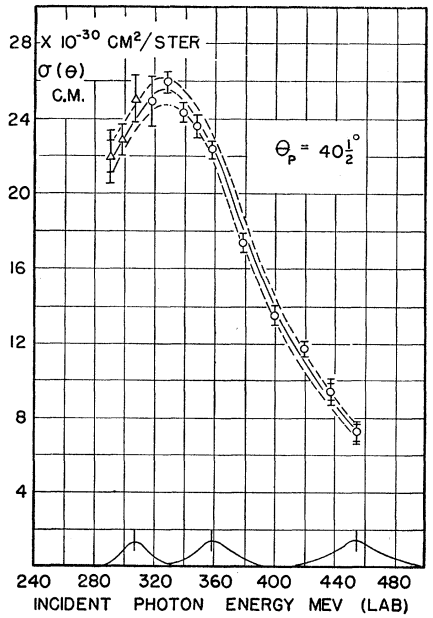

FIG. 6. Excitation function at 40.5° (lab).

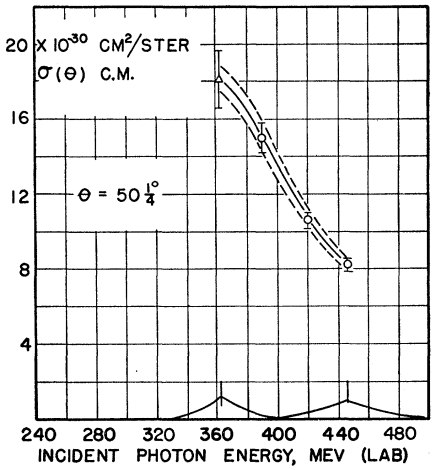

FIG. 7. Excitation function at 50.3° (lab).

indicate estimated systematic errors with the exception of systematic errors which affect only the overall absolute values of the cross sections. See the section on errors.

The angular distributions for constant photon energy can be found from the excitation functions by applying the relativistic angle transformation formulas. They are shown in Fig. 8 with a logarithmic ordinate and are tabulated in Table I. The center-of-mass angular resolutions are shown at the bottom of Fig. 8 with linear ordinate. The angular distributions have been fitted to the form $\sigma(\theta)=A+B\cos\theta+C\cos^2\theta$ by the method of least squares, and the resulting values of the coefficients A, B, and C are shown in Fig. 9.

Since the data do not extend forward of 10° at any energy, there is little experimental evidence that the cross section has the shape assumed, with only the three coefficients, A, B, and C. However, the assumption that only s- and p-wave mesons are produced appreciably in this energy region seems generally successful,

TABLE I. Angular distribution in c.m. system. $\sigma(\theta)$ is in units of 10^{-30} cm²/sterad.

		12.5° lab	19.5° lab	29° lab	40.5° lab	50.3° lab
270 Mev	$\sigma(\theta)$	8.1 ±1.3	10.5 ±0.6	15.1 ±0.5		
	θ_π	153°	136°	114°		
295 Mev	$\sigma(\theta)$	11.3 ±1.2	15.5 ±0.6	21.2 ±0.5	22.4 ±0.9	
	θ_π	153°	137°	115°	89°	
320 Mev	$\sigma(\theta)$	10.9 ±0.8	17.3 ±0.6	23.3 ±0.6	25.6 ±0.6	
	θ_π	153°	137°	115°	90°	
360 Mev	$\sigma(\theta)$	7.2 ±0.6	12.9 ±0.6	17.8 ±0.6	22.0 ±0.6	18.2 ±1.5
	θ_π	153°	138°	116°	91°	70°
400 Mev	$\sigma(\theta)$	3.6 ±0.4	7.6 ±0.4	10.9 ±0.5	14.1 ±0.5	13.6 ±0.6
	θ_π	153°	138°	117°	92°	71°
450 Mev	$\sigma(\theta)$	2.1 ±0.4	3.4 ±0.3	6.4 ±0.3	7.8 ±0.5	8.1 ±0.4
	θ_π	153°	138°	117°	93°	72°

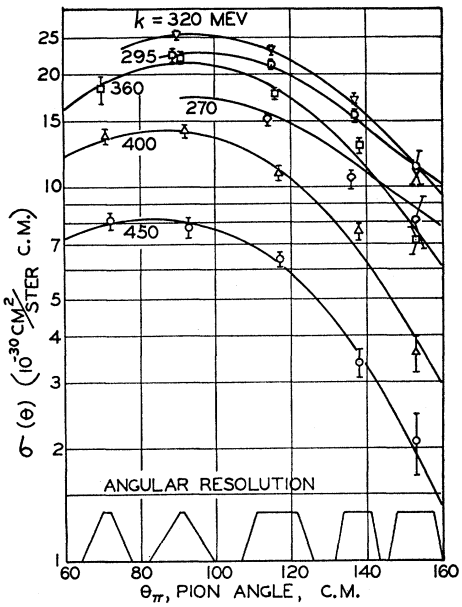

FIG. 8. Angular distributions for the reaction $\gamma+p\rightarrow p+\pi^0$. The differential cross section in the center-of-momentum system as a function of the c.m. pion angle for various laboratory photon energies.

and the more extensive data on positive pion production indicate no need for higher powers of $\cos\theta$ than the second. The values obtained for B and C depend, of course, on the form assumed for the cross section.

The simple least-squares analysis gives coefficients

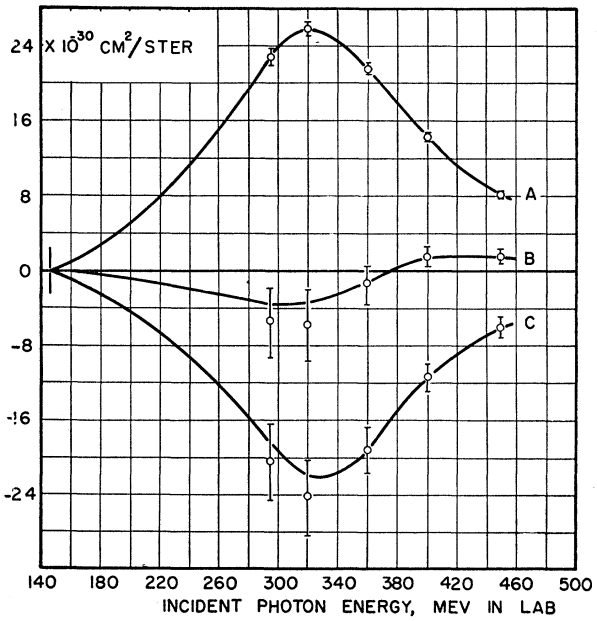

FIG. 9. Coefficients A, B, and C from a least-squares fit of the angular distributions to the form $\sigma(\theta)=A+B\cos\theta+C\cos^2\theta$ in the c.m. system. The solid curves have been drawn a little above the least-squares value at 295 and 320 Mev since the latter give negative cross sections at 0°.

B and C which at 295 and 320 Mev are impossible since they give negative cross sections at 0°. The solid curves in Fig. 9 have been drawn above the points (but within the indicated errors) so as to satisfy the requirement that the cross sections are nowhere negative. The curves have been extrapolated to threshold with a $(E_\gamma - E_T)^{\frac{3}{2}}$ energy dependence. The solid curves of Fig. 8 are computed from the coefficients A, B, and C corresponding to the solid curves of Fig. 9.

The total cross section, computed from the coefficients A and C given by the solid curves of Fig. 9, is given in Table II, and in Fig. 13. The total cross section divided by the square of the c.m. photon-wavelength is given in Fig. 10.

ELASTIC SCATTERING

Since only the recoil proton is observed in this experiment, the question arises whether protons may be produced from hydrogen by other processes than neutral pion production. One possible source of protons is, of course, elastic scattering of the photons in hydrogen. Since no mass is created in this process the relation between photon energy and proton angle and energy is different from the corresponding relation for photopion production, and this offers a possible means to distinguish between the two processes. Figure 11 shows data taken in an attempt to show that protons produced in elastic scattering are negligible. The insert in Fig. 11 shows a portion of the dynamics of the two reactions, i.e., values of the proton energy, T_p and lab angle θ_p, for incident photon energies of 250, 300, 350, and 400 Mev. The rectangle in this insert shows the regions of T_p and θ_p accepted by the spectrometer while taking these data. From the position of the photon energy lines, it is clear that the sensitivity of the spectrometer to elastic scattered protons from 310-Mev photons is the same as the sensitivity to neutral pion recoil protons from 350-Mev photons. Thus the ratio of the number of protons from elastically scattered 310-Mev photons to the number of recoil protons from neutral pion photoproduction at 350 Mev must be less than or equal to the ratio of the numbers of counts obtained with peak synchrotron energies of 310 and 350 Mev. This ratio is $\leq 0.04 \pm 0.03$. Thus, within the accuracy of a few percent, elastic scattering does not introduce any error in the neutral pion cross section. (The proton "Compton cross section" is much smaller than the upper limit obtained here.)

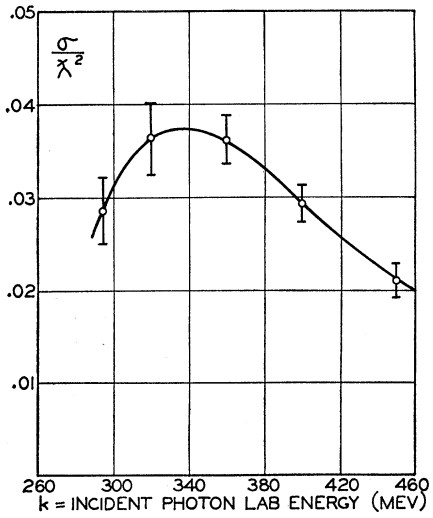

FIG. 10. Total cross section divided by $\lambda\!\!\!^{-2}$. $2\pi\lambda\!\!\!^{-}$ is the c.m. photon wavelength.

DATA REDUCTION

The center-of-mass differential cross section $\sigma(\theta)$ is found from the counting rate by the following formula:

$$C = \sigma(\theta) \frac{d\Omega'}{d\Omega} \Delta\Omega N_H A N(k) \Delta K.$$

C is the counting rate per standard beam monitor reading, corrected for background. (Accidentals were always negligible.) This counting rate was found from pulse-height spectra such as shown in Fig. 2, in which the proton pulses are separable from pulses causes by mesons and electrons. $d\Omega'/d\Omega$ is the ratio of c.m. to laboratory solid angle at the given laboratory angle and energy; $\Delta\Omega$ is the laboratory solid angle accepted by the spectrometer; N_H is the number of hydrogen atoms per square centimeter normal to the photon beam, determined by the wolfram slits, and the hydrogen density; A is a correction for absorption and scattering in the target, absorbers, air path, and scintillators; $N(k)$ is the number of photons of energy k per Mev, per standard beam monitor reading; Δk is the range of photon energies corresponding to the range of proton energies defined by the counters.

TABLE II. Total cross sections. The errors are obtained from the least-squares analysis of the angular distributions. Errors of type C are not included.

k(Mev lab)	295	320	360	400	450
$\sigma(10^{-30}$ cm$^2)$	209±25	232±25	191±14	131±8	77±6

The energy k of the photons responsible for the counting rate is obtained from the measured momentum of the protons and the laboratory angle of observation by converting the momentum to its corresponding energy, converting the energy into a residual range for the protons as they traverse the magnetic analyzer, adding the range of the material in the proton path between the target and the magnet (including the target wall and the hydrogen inside the target), converting the total residual range back into an energy for the proton inside the target, and then using the relativistic kinetics of the two-body problem to obtain the laboratory photon kinetic energy.

The number of photons of this energy per Mev per standard beam monitor reading depends upon the absolute calibration of the ion chamber monitor mentioned under "Apparatus," and upon the shape of the bremsstrahlung spectrum. The spectrum of the synchroton beam has been measured with a pair spectrometer, and found to have the theoretical shape within the experimental accuracy of a few percent.[19]

To obtain the appropriate interval of photon energies, Δk, it is necessary to find the interval of proton energies at the point of production corresponding to the interval of momenta accepted by the spectrometer after the protons have passed through the target wall, any carbon absorbers, and air. This is done by converting the interval of momenta to an interval of proton energies at the spectrometer energy and then converting this to an interval of proton energies at the point of production by multiplying by the ratio of specific ionization at the production energy to that at the spectrometer energy.

The correction for absorption and scattering in the target, absorbers, air path, and scintillators used the theory of Fernbach, Serber, and Taylor[22] with the energy-dependent parameters determined by Taylor[23] for the nuclear absorption by the materials in the proton beam. The nuclear scattering cross sections were obtained by subtracting the absorption cross sections from the observed total cross sections reported in Rossi's book.[24] Coulomb multiple scattering was found to be negligible from the scintillators, air path, and carbon absorbers and the scattering-out from the target wall was assumed compensated by scattering-in.

The Coulomb multiple scattering in the carbon absorbers was checked by comparing cross sections obtained by using absorbers of aluminum, copper and lead. From the differences in these cross sections, the predicted loss from the carbon absorbers never exceeded 0.1 percent. This effect has been ignored and no error assigned to it.

ERRORS

The errors in the experiment may be classified into three types:

(A) *Random statistical errors*, indicated on the measured points in Figs. 3 to 7. These are mainly the counting statistics and an estimate of the error in separating the proton peak from the pion peak. However, they also include about 2 percent error from the reproducibility of reading the target density, the uncertainty in resetting the magnetic analyzer field, and fluctuations in the beam monitoring.

(B) *Systematic errors which vary smoothly* from point-to-point on an excitation curve or angular distribution. These errors are indicated by the dashed curves on either side of the excitation curves of Figs. 3 to 7.

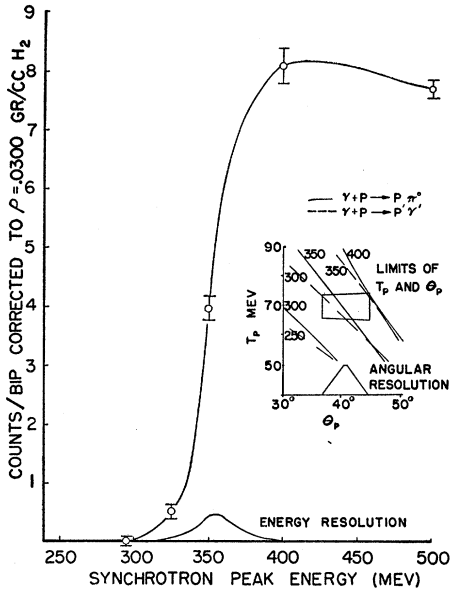

FIG. 11. Counting rate as a function of synchrotron energy, with the spectrometer set to count 70-Mev protons at 40.5°. See discussion in the section on Elastic Scattering.

They include the following: (1) Target wall thickness: 5 percent of thickness. (2) Absorber thickness: 1 percent of thickness. (3) Error in absorber scattering and absorption correction: 10 percent of the correction. (4) Slit penetration: 0 to 2 percent. (5) Error in proton angle setting: $\frac{1}{4}$ degree except at 12.5°, where it is 1 degree. (6) Beam monitor stability: 1.5 percent. (7) Uncertainty in the solid angle because the counters are not quite high enough to catch all the particles which get through the vertical aperture: 3 percent for long-focus measurements only.

A correction to the aperture solid angle was determined for the long-focus arrangement by comparing the counting rate with a 2-inch vertical aperture to that with the standard 3-inch aperture. The correction thus determined was 5.8±2.9 percent. No correction is necessary for the short-focus measurements because of partial vertical focusing in the fringe field of the magnet.

(8) Scattering from the lead shielding: The first set of runs was made with the lead "bridges" in Fig. 1 in a position very close to the particle paths. These runs did not show good consistency in the lower energies and investigation indicated that protons were scattering from the lead bridges in such a manner that they contributed to the counting rate, increasing the apparent cross section. The second set of runs tried to correct this effect by moving the bridges as far from the proton beam as was practical, to the position shown in Fig. 1. The bridges could not be dispensed with, because of increased background. The 12.5° measurements used bridges stacked of 2-inch lead bricks alternating with 2-inch air spaces from the

[22] Fernbach, Serber, and Taylor, Phys. Rev. **75**, 1352 (1949).
[23] T. B. Taylor, Phys. Rev. **92**, 831 (1953).
[24] Bruno Rossi, *High Energy Particles* (Prentice-Hall, Inc., New York, 1952), p. 344.

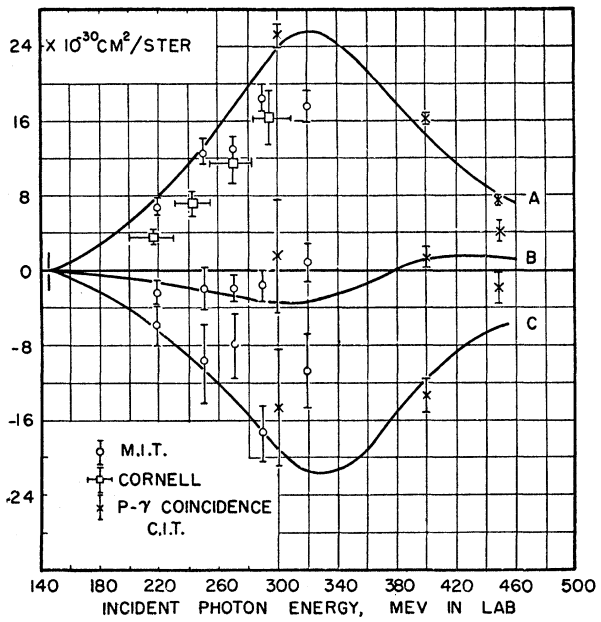

FIG. 12. Comparison with other experiments. The solid curves are the same as in Fig. 9 and represent the results of the present experiment. The data of Silverman and Stearns (see reference 3) at Cornell University are shown by the squares. Data from the Massachusetts Institute of Technology by Goldschmidt-Clermont, Osborne, and Scott (see reference 5) are shown by circles. The crosses are our older data obtained by measuring p-γ coincidences (see reference 16).

magnet to the target on one side and a solid wall of lead $\frac{2}{3}$ of the way from the magnet to the target on the other side. The other angles used solid bridges on both sides of the beam, so the corrections determined for these angles could not be applied directly to the 12.5° data, which were not repeated. Therefore, these data are reported as observed, but the correction factors are included in the estimate of the systematic errors shown by the dotted lines in Fig. 3.

(C) *Errors in the absolute cross sections*, independent of proton angle and energy. These amount to about 8 percent, and are not indicated in any of the figures. They include the following: (1) Error in the absolute beam calibration: 7 percent. (2) Error in the momentum range, Δp, accepted by the spectrometer: 2 percent. (3) Average target gas density: 2 percent.

COMPARISON WITH OTHER EXPERIMENTS

Data from other experiments are shown in Fig. 12, together with the same curves as in Fig. 9, obtained from this experiment. The old data of Silverman and Stearns[3] from Cornell University are considerably lower in value, but not by much more than the 30 percent quoted error in the absolute values.

The data from our older experiment using proton-γ coincidences[16] are indicated by the crosses in Fig. 12, and agree rather well with the present data.

The recently reported photographic plate results of Goldschmidt-Clermont, Osborne, and Scott[5] from the Massachusetts Institute of Technology are shown by the circles in Fig. 12. They agree fairly well with the solid curve which is extrapolated from our higher energy data by a $(E_\gamma - E_T)^{\frac{3}{2}}$ dependence. The Massachusetts Institute of Technology data give slightly lower values than this solid curve, but the worst discrepancy, at 320 Mev, is perhaps a result of the difficulties in obtaining data so near the upper end of the Massachusetts Institute of Technology bremsstrahlung spectrum.

Recent measurements in this laboratory[25] using a counter telescope to measure the recoil protons give preliminary results perhaps 10 percent lower than the present measurements in the region of the peak.

INTERPRETATION

As mentioned in the introduction, an analysis of photomeson production in terms of any theory is best done by considering charged and neutral production together. Such an analysis is being prepared in collaboration with K. M. Watson, based on his extension[14] of the phenomenological description of Gell-Mann and Watson.[11] For this reason only the most striking features of the data will be discussed here, namely the energy dependence of the cross section, and the angular distribution, which is rather independent of energy.

If one makes the assumption[8] that neutral pion photoproduction takes place mainly through a state of angular momentum $J=\frac{3}{2}$ and isotopic spin $T=\frac{3}{2}$ and that the production into s states is small, then the energy dependence near threshold[8,9] should be approximately like η^3, where η is the momentum of the pion in the c.m. system in units of the pion mass μ. At higher energies, the energy dependence of the matrix elements for production into the $J=\frac{3}{2}$, $T=\frac{3}{2}$ state becomes important. The approximate energy dependence of these "enhanced" matrix elements has been given by Watson,[10,26] and by Chew,[13] and may be expressed by a factor $\eta^{-2}\sin\alpha_{33}$, where α_{33} is the pion-nucleon scattering phase shift in the $J=\frac{3}{2}$, $T=\frac{3}{2}$ state. An estimate for the energy dependence of the c.m. cross section is obtained by multiplying the square of $\eta^{-2}\sin\alpha_{33}$ by a factor $\eta\omega E_f(\omega+E_f)^{-1}$ from the density of states, and dividing by the incident flux $c(1+\nu/E_i)$. $\omega=(\eta^2+1)^{\frac{1}{2}}$ is the pion energy, ν the photon momentum, and E_f the final nucleon energy, all in the c.m. system in units of the pion mass μ.

The resulting estimate is approximately (within one or two factors of ν or ω)

$$\sigma_{\text{est}}=N\left(1+\frac{\nu}{M}\right)^{-2}\eta^{-3}\sin^2\alpha_{33}.$$

[25] R. Smythe and R. M. Worlock, Bull. Am. Phys. Soc. **29**, No. 8, 21 (1954).
[26] K. M. Watson, Phys. Rev. **88**, 1163 (1952).

This function is shown in Fig. 13 for the scattering phase shift α_{33} chosen by Bethe and de Hoffman.[27] For comparison, the measured total cross section obtained from the coefficients A and C of Fig. 9 is also plotted in Fig. 13. The agreement at low energies is not very significant, of course, since the "measured" curve has also been given an energy dependence in this region expected from theory. However, the data of Silverman and Stearns,[3] and of Goldschmidt-Clermont, Osborn, and Scott[5] indicate that this energy dependence is about right.

At high energies, above 350 Mev, the estimated cross section falls off more rapidly than the measured one. This difference may be reduced by including in the analysis contributions from other p state matrix elements than the enhanced $J=T=\frac{3}{2}$ ones.[14] However, even the simple analysis above shows that the rapid decrease in the cross section above 340 Mev, which is faster than the decrease in λ^2, as shown in Fig. 10, is explained quite simply by the idea of a resonance in the $J=T=\frac{3}{2}$ state. The resonance is indicated, of course, by the phase shift α_{33} going through 90° in the analysis of Bethe and de Hoffman.[27]

The angular distribution, Fig. 8, is rather independent of energy. The coefficient B is small, and the ratio $-A/C$ is 1.22 ± 0.10 at all energies from 295 to 450 Mev. If π^0 production took place solely by magnetic dipole absorption into the $J=\frac{3}{2}$, $T=\frac{3}{2}$ state, the ratio $-A/C$ would be 1.67 so experiment shows that other matrix elements are also involved, which is not surprising. Perhaps the most important is that for electric quadrupole absorption into the same pion-nucleon state.

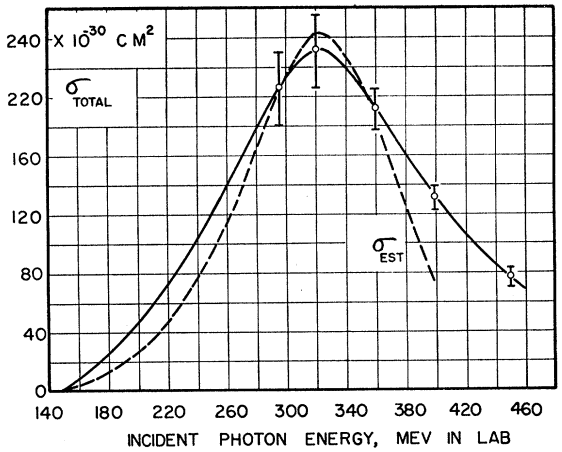

FIG. 13. The total cross section σ obtained from the present experiment, compared to an estimated energy dependence, σ_{est}, described under "Interpretation".

ACKNOWLEDGMENTS

We are considerably indebted to Michel Bloch, Paul Donoho, James Vette, and Dr. John G. Teasdale for helping to take some of the data, and to Professor R. F. Bacher for continued interest in the experiment, and many discussions about it.

[27] H. A. Bethe and F. de Hoffman, Phys. Rev. **95**, 1100 (1954).